www.sciencemag.org/cgi/content/full/science.aac7049/DC1

Supplementary Materials for

RNA editing by ADAR1 prevents MDA5 sensing of endogenous dsRNA as nonself

Brian J. Liddicoat, Robert Piskol, Alistair M. Chalk, Gokul Ramaswami, Miyoko Higuchi, Jochen C. Hartner, Jin Billy Li, Peter H. Seeburg, Carl R. Walkley*

*Corresponding author. E-mail: cwalkley@svi.edu.au

Published 23 July 2015 on *Science* Express
DOI: 10.1126/science.aac7049

This PDF file includes:

Other Supplementary Material for this manuscript includes the following:
(available at www.sciencemag.org/cgi/content/full/science.aac7049/DC1)

Tables S1 to S4 (Excel files)

Materials and Methods

Mice

All animal experiments were approved by the St. Vincent's Hospital, Melbourne AEC. *Adar1*^{E861A} mice were generated by Taconic Biosciences GmbH (Köln, Germany). The targeting vector was generated using BAC clones from the C57BL/6J RPCI-23 BAC library and was transfected into Taconic Biosciences C57BL/6N Tac ES cell line. Gene targeting was performed in the Taconic Biosciences C57BL/6N Tac ES cell line to generate constitutive knock-in of *Adar1*$^{E861A/+}$ allele (Fig. 1A). Homologous recombinant clones were isolated using positive (PuroR) and negative (Thymidine kinase - Tk) selection. Positive clones were selected and expanded then screened by Southern blot for correct targeting events. A correctly target ES line was used to generate chimeras. Chimerism was measured in chimeras (G0) by coat color contribution of ES cells to the BALB/c host (black/white). Highly chimeric mice were bred to strain Flp-Deleter C57BL/6 females (C57BL/6-Tg$^{(CAG\text{-}Flpe)2\ Arte}$) (*23*). Genotyping was performed by PCR using primers: 5'-TACTTGCAAGCATGCTGTGC-3' and 5'-TGCTACCCATATGTCAGCTGC-3' to yield products of 355bp (WT) and 446bp for KI allele. All PCR products were sequence confirmed.

Ifih1$^{-/-}$ (MDA5$^{-/-}$, B6.Cg-*Ifih1*$^{tm1.1Cln}$/J; stock number 015812) mice were purchased from Jackson Laboratory on a C57BL/6 background and genotyped as described by Jackson Laboratory (*24*). h*Scl*-CreER^{T}, *Adar1*$^{fl/fl}$ and *Rosa26*-CreER^{T2} mice have been previously described (*6, 25, 26*). All lines were on a C57BL/6 background. Tamoxifen containing food was prepared at 400mg/kg tamoxifen citrate (Sigma) in standard mouse chow (Specialty Feeds, Western Australia).

Monoclonal antibody and western blot

A cDNA fragment encoding the 400aa murine ADAR1 fragment (744-1944aa) with a 5' HIS tag (Fig. S1B) and cloned into the prokaryotic expression vector pET-16b. The construct was expressed in BL-21 competent *E.coli* (New England Biolabs) and protein was purified using TALON metal affinity resins (Clontech Laboratories). Rats were immunized with purified protein and hybridoma cell lines cloned (Monash Antibody Technologies Facility, Monash University, Clayton, Victoria, Australia). anti-ADAR1

monoclonal antibody was purified from hybridoma supernatant using MAb Trap Kit (GE Healthcare). Specificity of monoclonal antibody was demonstrated by western blot using *Adar1*$^{+/-}$ (control) and *Adar1*$^{-/-}$ whole embryo protein preparations (Fig. S1F). Clone RD4B11 was further expanded and used subsequently. SDS-PAGE was carried out with 10% Bis-tris precast gels (Invitrogen) and transferred to nitrocellulose filter membranes (Millipore) using XCell II blot module (Invitrogen) as per manufacturers instructions. 1mg/mL purified monoclonal antibody was used to probe nitrocellulose membranes for western blot analysis.

Flow cytometry analysis

Peripheral blood was analyzed on a hematological analyzer (Sysmex KX-21N, Roche Diagnostics). Single cell fetal liver suspensions were prepared by passing through a 23g needle. Bones were flushed, spleens and thymus crushed and single cell suspensions were prepared. Antibodies against murine Ter119, CD71, B220, IgM, Mac-1, Gr1, F4/80, CD43, CD19, CD4, CD8, CD44, Sca-1, c-Kit, CD34, FLT3, FcγR (CD16/32), CD41, CD48, CD51, either biotinylated or conjugated with FITC, PE, PE-Cy5, PerCP-Cy5.5, PE-Cy7, APC or APC-eF780 were all obtained from eBioscience. CD105 and CD150 were from BioLegend. Biotinylated antibodies were detected with streptavidin conjugated with Brilliant Violet-605 (Biolegend). AnnexinV (BD) and 7-AAD (Molecular Probes) was used to assess viability. Cells were sorted on a BD FACSAria or BDInflux cell sorter and analyzed on a BD LSRIIFortessa (BD Biosciences). Results were analyzed with FlowJo software Versions 9.4.11 and X.0.7 (Treestar).

RNA-Seq

Total RNA from three individual *Adar1*$^{+/+}$ and *Adar1*$^{E861A/E861A}$ FL, E12.5 embryo littermates were sequenced on the Illumina HiSeq 2000 with 100bp paired-end reads at The Ramaciotti Centre for Genomics, UNSW, Australia. Raw sequencing data is deposited in GEO (GSE58917).

Mapping, variant calling and identification of differentially edited sites

RNA-seq reads were aligned to the MM9/NCBIM37 reference genome with BWA (*27*). A-to-I(G) editing sites were determined as previously described (*3*). Briefly, paired-end reads were mapped separately to mm9 reference genome and exonic sequences encompassing known splicing junctions. PCR duplicates were removed and unique reads were subjected to local realignment. Variants were called and reported at lenient call criteria (stand_call_conf 0, stand_emit_conf 0). Variants were removed from the resulting candidate list if they overlapped with known genomic variation, had a variant call quality <20 or were located in the first six bases of a read, within 4bp of a splice junction, in homopolymer runs or in simple repeats. Editing level at each of these sites was quantified. Editing sites in hyper-edited regions were identified as previously described (*28*).

Differential gene expression analysis (RNA-seq)

We used a differential expression analysis pipeline developed at the Life Sciences Computation Centre, VLSCI, University of Melbourne. The pipeline is based on the Tuxedo protocol (Tophat, Cufflinks) and EdgeR/Voom with HTSeq-count (Source code available at: https://bitbucket.org/jessicachung/rna_seq_pipeline). Aligned reads (see above) were summarised using HTSeq (*29*). Normalization factors were calculated using the edgeR method="TMM" corresponding to the weighted trimmed mean of M-values (to the reference) (*30*), where the weights are from the delta method on Binomial data. Normalized read counts (moderated log counts per million) and differential expression were generated using a protocol from Voom (*31*).

Data normalization and analysis of *Adar1*$^{-/-}$ HSCs

Raw data was downloaded from GEO (GSE12772) and processed in GenePattern (*32*) using ExpressionFileCreator to perform background correction and quantile normalization on the data. Only *Adar1*$^{+/+}$ and *Adar1*$^{-/-}$ samples were used. Probes that were not detected in all *Adar1*$^{+/+}$ or all *Adar1*$^{-/-}$ samples were discarded (leaving 10,687 probes). The data was collapsed to gene level, leaving 4,642 genes for gene set analysis.

Gene set analysis

Quantitative Set Analysis for Gene Expression (QuSAGE) was performed as described (*33*) on both ADAR1^{E861A} and GSE12772 datasets against the MSigDB collection "C2:curated gene sets" (c2.cgp.v4.0) (*34*) and the IU-dsRNA responsive gene set (*13*).

RNA secondary structure prediction

Genomic sequences from Ensembl Genes 75, Mus musculus genes (GRCm38.p2) were used to predict RNA secondary structures using the mfold web server as previously described (*35*), RNAfold version 3.0 with default settings. To predict RNA secondary structures of edited transcripts, 'A's' were placed with 'I's' in genomic sequences at A-to-I sites identified in the RNA-seq dataset prior RNAfold analysis.

Validation of A-to-I editing sites

RNA was isolated from 3 independent *Adar1*$^{E861A/E861A}$ and *Adar1*$^{+/+}$ FL and mouse embryonic fibroblasts (MEFs) cell lines at passage 2 using Trisure (Bioline). cDNA was synthesized with AffinityScript reverse transcriptase (Agilent). Edited sites were validated using independent samples by Sanger sequencing. Primer sequences are listed below. 281 sites were validated sites using a microfluidic multiplex PCR (mmPCR) sequencing method on independent FL and MEF samples from 3 *Adar1*$^{+/+}$ and 3 *Adar1*$^{E861A/E861A}$ E12.5 embryos (*15*). 200ng of cDNA was used for mmPCR-seq. Briefly, 557 loci containing 11,103 known A-to-I editing sites (Tan *et al.* unpublished data) were PCR amplified using multiplexed primer pools. PCR amplicons were used for high throughput sequencing and A-to-I editing frequencies were determined as described in the methods.

Primer Sequences used for Sanger Sequencing

Gene	Forward *	Reverse	Product Size (bp)
Blcap	5'-CTGACAGCCAGAGAGCACAG-3'	5'-ATTGTGCAAGGTTTCCGTTC-3'	281
Mad2l1	5'-AATTTTCCGGTGAAGAAAGC-3'	5'-AGCTTTGATCCCTTCTGCTG-3'	279
Rpa1	5'-CTCAGAGGGCTGTGTGTGAA-3'	5'-AGACAAAAAGGTGCCACCAC-3'	214
Klf1	5'-ACCCTCAAGGCCAGCTAGA-3'	5'-ATTCCAGCATCCTCTGCACT-3'	332
Adar1	5'-CCCAGACTGTCAGCTCAAGG-3'	5'-AGGACTCGGGTCATTCAGG-3'	316

* Used forward primer for Sanger sequencing

Knockdown of MDA5 with shRNA

LKS^+ were isolated as previously described (*36*). 5 x 10^4 LKS^+ cells were infected with pLKO shRNA targeting MDA5, RIG-I (Sigma) or a control shRNA targeting GFP (Addgene) with an MOI of 2. Targeting sequences are:

shMDA5(1): 5′-CCACAGAATCAGACACAAGTT-3′ (TRCN0000103646)

shMDA5(2): 5′-GCAAAGCAATACAACGACAAT-3′ (TRCN0000103647)

shRIG-I: 5'-CCACAGTTGATCCAAATGATA-3' (TRCN0000103886)

shGFP, 5′-GCAAGCTGACCCTGAAGTTCAT-3′ (Plasmid 30323).

Lentivirus production and infection procedures were performed using standard procedures. Following infection, the cells were cultured in a selection medium containing 2μg/ml puromycin for 3 days to enrich infected cells before experiments were performed.

Primer Sequences used for RT-qPCR

Gene	Forward	Reverse	Product Size (bp)
RIG-I	5'-AAAGACGGTTCACCGCATAC-3'	5'-TCTTGCACTTTCCACACAGC-3'	113
MDA5	5'-TCACTGATCTGCCCTCTCCT-3'	5'-CCTTCTCGAAGCAAGTGTCC-3'	129
Irf7	5'-CCAGTTGATCCGCATAAGGT-3'	5'-AGCATTGCTGAGGCTCACTT-3'	99
Ifit1	5'-ATGGGAGAGAATGCTGATGG-3'	5'-AGGAACTGGACCTGCTCTGA-3'	137
Tgtp	5'-AGCATTAGCCACCATTCCAC-3'	5'-TTCCAGTGAAGCATCATCCA-3'	112
Adar1p110	5'-GGTGGAAGACTACGCGTTGGGAC-3'	5'-ACGACTGTGTCTGGTGAGGGAACAC-3'	112
Adar1p150	5'-GGCCTTGCCGGCACTATGTCTC-3'	5'-GCGGGTATCTCCACTTGCTATGCTC-3'	112

Statistical analysis

For biological experiments, the significance of results was analyzed using the unpaired two-tailed student T-test on the bases that highly inbred genetically identical mice have been used in all experiments, $p<0.05$ was considered significant. All data are depicted as means±S.E.M.

The significance of differential editing levels was determined using one-way ANOVA, based on the assumption that the populations were Gaussian, $p<0.1$ was considered significant. All data represented as the mean.

Supplementary Text

Specific loss of ADAR1-mediated A-to-I editing results in embryonic death

To elucidate the specific contribution of A-to-I editing by ADAR1, we generated mice with a constitutive knock-in of an editing-deficient (*Adar1*^{E861A}) point mutation (Fig. 1A). Sequencing of exon 9 demonstrated successful transmission of the *Adar1*^{E861A} allele (Fig. S1A). To confirm that the ADAR1^{E861A} protein was expressed, we generated a monoclonal antibody against murine ADAR1 (Fig. S1B). The constitutive ADAR1p110 isoform was detected in *Adar1*$^{E861A/E861A}$ samples at levels similar to *Adar1*$^{+/+}$ and *Adar1*$^{E861A/+}$ controls. However, *Adar1*$^{E861A/E861A}$ samples also contained very high levels of the interferon (IFN)-inducible ADAR1p150 isoform (Fig. 1B), suggestive of an activated IFN response in mutant embryos. *Adar1*$^{E861A/+}$ heterozygous mice were normal, fertile and had no discernible phenotype, similar to ADAR1 heterozygous null (*Adar1*$^{+/-}$) animals (*6, 7*). Whole original western blot images are shown in Fig. S1C.

A-to-I editing by ADAR1 is required for the maintenance of fetal hematopoiesis

ADAR1 is dispensable for the developmental emergence of hematopoietic stem cells (HSCs), but absolutely required for the maintenance of hematopoiesis (*12*). To determine if A-to-I editing was necessary for this function of ADAR1, immunophenotyping of FL hematopoietic cells from viable E13.5 *Adar1*$^{E861A/E861A}$ embryos was undertaken. Editing was absolutely required for normal erythropoiesis (Fig. 1E-G). There was a severe loss of erythroblast populations (R2-R4), encompassing proerythroblasts through to reticulocytes, in the *Adar1*$^{E861A/E861A}$ FL (Fig. 1F). Cell death was not restricted to erythroblasts, as mature leukocytes (lineage$^+$), lineage$^-$c-Kit$^+$Sca1$^-$ (LKS$^-$) and lineage$^-$c-Kit$^+$Sca1$^+$ (LKS$^+$), multipotential progenitor (MPP) and HSCs also had significantly increased frequencies of 7AAD$^+$ cells in *Adar1*$^{E861A/E861A}$ compared to wild-type FL (Fig. S2A).

Amongst more primitive populations, the percentage of the HSC-enriched LKS$^+$ cells was ~3-fold greater in *Adar1*$^{E861A/E861A}$ FL compared to controls (Fig. S2B-C). However the absolute numbers (Fig. S2D) were reduced due to decreased FL cellularity (Fig. S1E). Conversely, both the frequency and absolute number (Fig. S2B-D) of the progenitor containing LKS$^-$ population were reduced by >10-fold in *Adar1*$^{E861A/E861A}$ FL.

We noted 3-fold higher cell surface expression of Sca-1, an IFN-inducible protein, in *Adar1*$^{E861A/E861A}$ cells (Fig. S2E), consistent with the ectopic expression of ADAR1p150 in the embryos (Fig. 1B), indicative of an activated IFN response in FL. This phenomena was previously reported in the *Adar1*$^{-/-}$ FL (*12*).

To quantitate long-term HSCs in FL we evaluated the LKS^{+}CD48^{-}CD150^{+} population (*37*). Whilst the frequency of HSCs was higher in *Adar1*$^{E861A/E861A}$ FL than controls (Fig. S2F), the absolute number was similar to controls (Fig. S2G) as a result of decreased FL cellularity (Fig. S1E). Both the frequency and number of LKS^{+}CD48^{-} CD150^{-} multipotent progenitors (MPP) was significantly reduced in the *Adar1*$^{E861A/E861A}$ FL (Fig. S2F-G). In contrast, LKS^{+}CD48^{+}CD150^{-} lineage-restricted progenitor (LRP) frequency and number remained largely unchanged (Fig. S2F-G). The percentage of dead HSC and MPP fractions was significantly elevated, whereas viability of the LRPs was unchanged (Fig. S2A). At E12.5 the *Adar1*$^{E861A/E861A}$ FL had a near absence of mixed and erythroid colony forming units (CFU) compared to controls (Fig. S2H). Although myeloid CFUs were present, both numbers and colony size were reduced (Fig. S2H-I). These data demonstrate that A-to-I editing by ADAR1 is essential for the maintenance of HSCs and MPPs, but dispensable for the emergence of HSCs. Collectively these data demonstrate that RNA editing by ADAR1 is essential for fetal hematopoiesis.

ADAR1-mediated A-to-I editing is required for adult hematopoiesis

To assess the requirement for editing by ADAR1 in adult hematopoiesis, mice with a tamoxifen-inducible CreER^{T} transgene driven by the hematopoietic enhancer of the *Scl* promoter (h*Scl*-CreER^{T}) (*25*) and homozygous for the ADAR1 loxP-flanked (*Adar1*^{fl}) allele (*6*) were crossed with *Adar1*$^{E861A/+}$ mice. In the presence of tamoxifen, h*Scl*-CreER^{T}*Adar1*$^{fl/E861A}$ mice (termed HSC-*Adar1Δ/E861A* here) deleted the wild-type floxed ADAR1 allele and retained only the editing deficient allele. Results were compared to tamoxifen treated h*Scl*-CreER^{T}*Adar1*$^{fl/+}$ controls (HSC- *Adar1Δ/+*).

To determine if ADAR1-mediated RNA editing was required for adult hematopoiesis, a cohort of HSC-*Adar1Δ/E861A* and control mice were placed on a tamoxfen containing diet for 30 days and peripheral blood (PB) was analyzed at days 20, 48, 128, and 282 (cohort 1, Fig. S3A). HSC-*Adar1Δ/E861A* mice were anemic (Fig. S3B)

within 20 days of addition of tamoxifen diet. PB showed a decrease in leukocyte (59%) and platelet (64%) counts respectively in HSC-*Adar1Δ/E861A* after 20 days of tamoxifen diet (Fig. S3B). Within 18 days of ceasing tamoxifen diet, PB leukocyte and platelet counts returned to control levels (Fig. S3B). Resolution of the anemia was delayed, with PB erythroid indices fully restored by 14 weeks post tamoxifen cessation (Fig. S3B). All PB parameters were stable thereafter (up to 282 days follow up). The recovery of hematopoiesis in HSC-*Adar1Δ/E861A* mutants resulted from selection against cells expressing only $Adar1^{E861A}$ (Fig. S3C), a phenomenon previously observed in $Adar1^{fl/fl}$ mice (*12*). Cells expressing only the $Adar1^{E861A}$ allele were diluted over time in HSC-*Adar1Δ/E861A* mice and were no longer detectable upon completion of the experiment, having been replaced by non-excised, wild-type ADAR1 expressing cells (Fig. S3C).

Given the loss of cells expressing $Adar1^{E861A}$, hematopoiesis was assessed immediately following cessation of tamoxifen (cohort 2, Fig. S3A). The bone marrow (BM) of HSC-*Adar1Δ/E861A* showed reduced cellularity compared to HSC-*Adar1Δ/+* mice (Fig. S3D). Again there was evidence of strong selection against excision of the $Adar1^{fl}$ allele in HSC-*Adar1Δ/E861A* mice (Fig. S3E), consistent with the PB. The frequency of LKS^+ cells was increased, whilst the LKS^- progenitors were reduced in HSC-*Adar1Δ/E861A* (Fig. S3F). Analysis of phenotypic long-term HSCs, short-term HSCs and MPPs, based on CD34 and CD135 expression (*38*), revealed a significant increase in all three populations in HSC-*Adar1Δ/E861A* mice (Fig. S3G). Conversely there was a 2-3-fold reduction in the number of the myelo-erythroid restricted progenitors (MEP, CMP, GMP) per femur (Fig. S3G). An alternative fractionation approach of the LKS^- population revealed consistently reduced numbers of pre-GM, pre-MegE, pre-CFU-E, CFU-E and MkP progenitors (*39*) in HSC-*Adar1Δ/E861A* BM (Fig. S3H). A 30% reduction of the committed erythroid populations likely caused the transient anemia in HSC-*Adar1Δ/E861A* mice (Fig. S3I). HSC-*Adar1Δ/E861A* whole BM and purified LKS^+ cells had significantly reduced CFUs (Fig. 3J). Selection against deletion of $Adar1^{fl}$ was consistently detected in HSC-*Adar1Δ/E861A* colonies, whereas CFUs derived from HSC-*Adar1Δ/+* animals maintained a stably excised floxed allele (Fig. S3J-K). These data

demonstrate that adult hematopoiesis cannot be maintained in the absence of ADAR1 catalyzed RNA editing.

Loss of ADAR1-mediated A-to-I editing leads to an upregulation of interferon signatures

ADAR1-mediated editing is essential for fetal and adult hematopoiesis (Fig. S2-S3). In order to determine the mechanism by which ADAR1-mediated RNA editing regulates hematopoiesis, we performed RNA sequencing on 3 independent littermate *Adar1*$^{+/+}$ and *Adar1*$^{E861A/E861A}$ E12.5 FL and assessed gene expression changes. We chose to perform RNA-seq on whole FL as we know that it is a tissue that requires ADAR1 editing. The E12.5 time point was chosen to obviate developmental and viability impacts on the dataset.

From the 50 most deregulated genes (Fig. 2C), transcription factor binding sites are defined for 33 of the 44 most upregulated ISGs, 30 of which have IFN regulatory factor 7 (IRF7) binding sites upstream of the transcription start site (Fig. S4A). We compared the overlap of differentially expressed genes with *Adar1*$^{-/-}$ HSCs, by reanalyzing microarray profiles from these cells (*12*). Only 36 of the 50 transcripts were annotated in the *Adar1*$^{-/-}$ HSCs dataset, yet 26 (72%) were also upregulated when compared to controls (Fig. S4B). Therefore the transcriptional response in *Adar1*$^{E861A/E861A}$ cells mirrors closely that of complete ADAR1 deficiency despite different populations of cells being assessed in each study (*12*).

The upregulation of ISGs was confirmed by qRT-PCR analysis of independent viable E12.5 FLs. Known IFN-inducible transcripts including *Tgtp*, *Ifit1*, *Irf7*, *Ddx58* (Retinoic acid-inducible gene I (RIG-I)) and *Ifih1* (melanoma differentiation-associated 5 (MDA5)), and *Adar1p150* itself were profoundly upregulated in *Adar1*$^{E861A/E861A}$ FL and mouse embryonic fibroblasts (MEFs, Fig. 2D). Both *Ifit1* and *Tgtp* were upregulated ~10^3-fold in *Adar1*$^{E861A/E861A}$ FL over controls, whereas these genes were only upregulated ~10-fold in passage 1 MEFs (Fig. 2D). We have previously reported that ADAR1 was not essential for embryonic stem cells or MEFs (*12*). MEFs derived from *Adar1*$^{E861A/E861A}$ embryos could be maintained *in vitro*, which may reflect a cell-specific requirement for ADAR1 editing.

Identification of ADAR1-specific editing sites in fetal liver

To define ADAR1 specific RNA editing events *in vivo*, we analyzed A-to-I (G) mismatches from RNA-seq data (Fig. 3). The FL was chosen as it is an organ in which we know ADAR1-mediated editing is essential (Fig. S2). The original 6,267 A-to-I editing sites were identified based on a published pipeline (*3*), which may include false-positives. Using stringent filtering criteria outlined in Fig. 3A, we identified a total of 418 high-confidence A-to-I sites that differed significantly between *Adar1*$^{E861A/E861A}$ and controls (Table S2). >20 reads was determined as a suitable cut-off for coverage over edited sites, based on significant R^2 values between biological replicates (Fig. S5). We noted the presence of 1 editing site within the 3'UTR of *Klf1*, which was of interest due its known role in erythropoiesis. Upon investigation of this site in the intergrated genome viewer (IGV), we observed 127 additional sites in an extended and unannotated 3'UTR of *Klf1* (Fig. 3D), which were not identified in the original analysis. These sites would not have been identified as they are located in repetitive regions. Therefore, an additional analysis method was applied to identify A-to-I sites within these hyperedited/repetitive regions (*28*). From this analysis, we identified an additional 255 (264 total) sites in just 3 genes: *Klf1*, *Optn* and *Oip5* (Table S3). 9 of these 264 sites overlapped with the original analysis (Table S2-S3). Due to the extensive editing found within these genes, we defined them as 'hyper-edited'. Combining the two analyses we identified 673, high-confidence A-to-I editing sites.

Unexpectedly, of the 673 A-to-I mismatches differentially edited, 7 showed increased editing in the *Adar1*$^{E861A/E861A}$ (Fig. 3B). These are known ADAR2 editing sites (*1*) and *Adar2* is expressed in the FL (Table S1). The remaining 666 A-to-I sites had effectively no detectable editing in the mutant, especially hyper-edited loci (Fig. 3B, Table S2-S3). This demonstrated that the majority of A-to-I editing in the FL is mediated by ADAR1 and confirms that the *Adar1*^{E861A} allele is truly catalytically inactive.

To validate the identified sites we performed microfluidics-based multiplex PCR with deep sequencing (mmPCR-seq) (*15*) on independent *Adar1*$^{E861A/E861A}$ and *Adar1*$^{+/+}$ FL and passage 2 MEFs samples. This method provided greater read coverage resulting in greater resolution of editing frequencies. For mmPCR-seq validation, the same filtering criteria from the original analysis was applied (Fig. 3A). A total of 1,512 sites

met these criteria using mmPCR-seq (Table S4). From these 1,512 sites, 281 overlapped with sites discovered *de novo* in the RNA-seq dataset and were confirmed as differentially edited in both FL and MEFs between *Adar1*$^{E861A/E861A}$ and controls (Table S4).

We next assessed the potential consequences of the absent editing event(s) in *Adar1*$^{E861A/E861A}$ cells. A-to-I editing in introns can alter splicing in a tissue specific manner (*40*). 30 A-to-I editing sites were located within the introns of 21 genes (Fig. 3A, Table S4). However, none of these edited sites are known acceptor splice sites. 3 ncRNAs were differentially edited (10 A-to-I sites total) and only 6 ADAR1-specific editing sites resulted in a predicted nonsynonymous codon change in 6 genes (Fig. 3A, Table S4). None of these transcripts have been implicated in hematopoiesis or regulation of IFN, hence they are unlikely to be critical to the manifestations of the *Adar1*$^{E861A/E861A}$ phenotype.

A potential consequence of editing in 3'UTRs could affect gene expression of targeted substrates. ADAR1 editing of 627 A-to-I sites in the 3' UTRs of 98 genes did not correlate with a deregulation in expression of the targeted transcripts in *Adar1*$^{E861A/E861A}$ FL (Fig. S6A). Only H2-T24 had a $Log_2FC>1.5$, and is a known ISG (Table S1). 70 editing sites were identified in the 3'UTR of the erythroid transcription factor *Klf1*, whose expression was 2-fold reduced in *Adar1*$^{E861A/E861A}$ FL (Fig. S6B). However, the decreased *Klf1* expression was likely secondary to failed erythropoiesis as both *Gata1* and *SCL*/*Tal1*, two key non-edited erythroid transcription factors, were decreased to an equivalent extent (Fig. S6B). 61 and 133 ADAR1-specific A-to-I sites within the long 3' UTRs of *Oip5 and Optn* respectively. By interrogating the Gene Expression Commons database (*41*) we found that the transcript expression of both *Optn* and *Klf1* markedly overlapped and was specific to erythroid progenitors (Table S3). *Oip5* is expressed throughout hematopoiesis, with peak expression in erythroid progenitors, providing a possible link to the FL failure observed in the embryos.

The hyper-editing in the 3'UTRs of *Klf1*, *Optn* and *Oip5* could act to destabilize long match stem loops (Fig. 3E, Fig. S7A-F). Conversely, 3'UTRs with less than five editing sites have predicted complex secondary structures and short dsRNA duplexes (Fig. S7G-I). Therefore, we hypothesized that RNA editing by ADAR1 remodels the

secondary structure of endogenous RNA to minimize the formation of long matched dsRNAs.

MDA5 knockdown rescues the hematopoietic defect of ADAR1^{E861A}

Short hairpin RNA (shRNA) was used to knockdown MDA5 and RIG-I in LKS^{+} cells, a hematopoietic cell population containing HSPCs, isolated from *Rosa26*-CreER^{T2}*Adar1*$^{fl/E861A}$ (LKS-*Adar1Δ/E861A*) and *Rosa26*-CreER^{T2}*Adar1*$^{fl/+}$ (LKS-*Adar1*Δ/+) control mice. Following tamoxifen treatment to delete the wild-type *Adar1*^{fl} allele, LKS-*Adar1Δ/E861A* cells would only have one intact copy of the *Adar1*^{E861A} allele. LKS-*Adar1Δ/E861A* cells and LKS-*Adar1*Δ/+ were transduced with two shRNA controls, both empty vector and shRNA targeting GFP (shGFP). The cell populations isolated do not express GFP and therefore the shGFP control is a non-specific target control. We used two independent shRNA to knock-down MDA5 (shMDA5(1) and shMDA5(2)). Both were confirmed to knock-down MDA5 (Fig. S8B). We demonstrated that MDA5 knockdown rescue of LKS-*Adar1Δ/E861A* cells was not due to selection against excision of the floxed allele (Fig. S8C).

Adar1$^{E861A/E861A}$ embryonic death is rescued by crossing to *Ifih1*$^{-/-}$ mice

Adar1$^{E861A/+}$*Ifih1*$^{-/-}$ intercrosses produced *Adar1*$^{E861A/E861A}$*Ifih1*$^{-/-}$ embryos at expected ratios (Fig. S9A). Yolk sac and embryo vascularization was also visually normal. At E13.5 *Adar1*$^{E861A/E861A}$ were smaller and appear developmentally delayed (Fig. 1D), whereas *Adar1*$^{E861A/E861A}$*Ifih1*$^{-/-}$ embryo proper were ostensibly normal (Fig. 4D). FL size, morphology and cellularity were comparable to controls (Fig. 4D, Fig. S9C).

FL erythropoiesis was completely rescued and was comparable to control littermates (Fig. 4E-F). Analysis of FL (Fig. 4G) and brain (Fig. S9D) ISG expression demonstrated that the derepression of *RIG-I*, *Irf7*, *Ifit1*, *Tgtp* and *Adar1p150* was reversed. *Ifit1* was increased ~3-fold in *Adar1*$^{E861A/E861A}$*Ifih1*$^{-/-}$ FL (Fig. 4G), however this is significantly lower than its expression in *Adar1*$^{E861A/E861A}$ FL at E12.5 (~1000-fold increase compared to controls, Fig. 2D). We also observed a subtle increase Sca1 expression on the surface of FL cells (Fig. S9E), indicative of an active IFN response in these cells, albeit at a significantly reduced magnitude than *Adar1*$^{E861A/E861A}$ embryos.

Although we observed a significant increase in LKS^{+} and lineage restricted progenitors (LRP) fractions, FL hematopoiesis was restored in *Adar1*$^{E861A/E861A}$*Ifih1*$^{-/-}$ embryos (Fig. S9F). Cell viability was also normal (Fig. S9G).

Most surprisingly, viable *Adar1*$^{E861A/E861A}$*Ifih1*$^{-/-}$ double mutants were identified that have survived >30 days (Fig. S9B). From 12 litters we expected 4 *Adar1*$^{E861A/E861A}$*Ifih1*$^{-/-}$, with 2 being identified at day 7-10 and both are >30 days of age. Both *Adar1*$^{E861A/E861A}$*Ifih1*$^{-/-}$ mice identified at 10 days of age based on standard genotyping have survived >30 days. We confirmed that the double mutant mice were homozygous for the *Adar1*^{E861A} allele by sequencing of the genotyping product (Fig. S9H).

We propose that ADAR1-mediated hyper-editing of self-dsRNA (such as *Klf1*, *Optn* and *Oip5* 3'UTRs) generates multiple I-U mismatches, preventing MDA5 oligomerization and therefore subsequent activation of downstream IFN signaling (Fig. S10). In the absence of ADAR1 editing, MDA5 forms oligomers along endogenous dsRNA, accrues mitochondrial antiviral-signaling protein (MAVS) filament formation, activates IRF7 and upregulates ISGs leading ultimately to cell death. From these studies we conclude that editing of endogenous RNA by ADAR1 prevents their recognition by the dsRNA innate immune system (Fig S10).

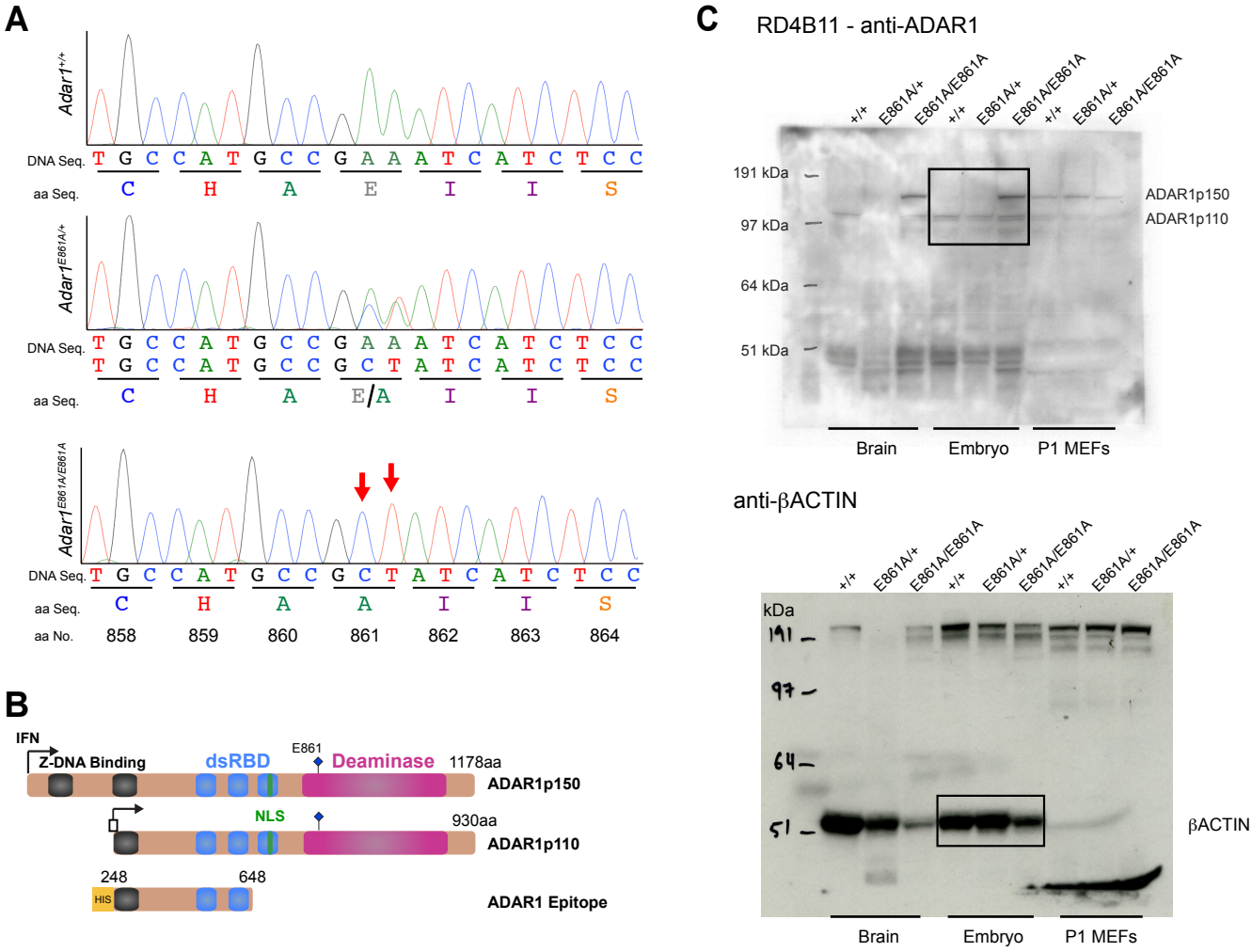
A
Adar1+/+
DNA Seq. T G C C A T G C C G A A A T C A T C T C C
aa Seq. C H A E I I S
Adar1E861A/+
DNA Seq. T G C C A T G C C G A A A T C A T C T C C
T G C C A T G C C G C T A T C A T C T C C
aa Seq. C H A E/A I I S
Adar1E861A/E861A
DNA Seq. T G C C A T G C C G C T A T C A T C T C C
aa Seq. C H A A I I S
aa No. 858 859 860 861 862 863 864
B
IFN
Z-DNA Binding
dsRBD
E861
Deaminase
1178aa
ADAR1p150
NLS
930aa
ADAR1p110
248
648
HIS
ADAR1 Epitope
C
RD4B11 - anti-ADAR1
+/+ E861A/+ E861A/E861A +/+ E861A/+ E861A/E861A +/+ E861A/+ E861A/E861A
191 kDa
97 kDa
64 kDa
51 kDa
ADAR1p150
ADAR1p110
Brain
Embryo
P1 MEFs
anti-βACTIN
+/+ E861A/+ E861A/E861A +/+ E861A/+ E861A/E861A +/+ E861A/+ E861A/E861A
kDa
191
97
64
51
βACTIN
Brain
Embryo
P1 MEFs
D
Adar1+/+
Adar1E861A/+
Adar1E861A/E861A
Embryo
E
+/+
E861A/+
E861A/E861A
Cellularity (x10⁶ / Liver)
10
8
6
4
2
0
p<0.0001
E12.5
E13.5
F
E11.0 Embryo
P1 MEFs
E12.5 Brain
+/- -/- E861A/+ E861A/E861A E861A/+ E861A/E861A
191 kDa
97 kDa
64 kDa
51 kDa
ADAR1p150
ADAR1p110
αTubulin

Figures S1-S10

Figure S1. ADAR1 monoclonal antibody and *Adar1*$^{E861A/E861A}$ phenotype

A) Exon 9 of *Adar1* was PCR amplified and representative Sanger sequencing traces for *Adar1*$^{+/+}$, *Adar1*$^{E861A/+}$ and *Adar1*$^{E861A/E861A}$ derived gDNA are illustrated. **B**) Schematic representation of the two isoforms of ADAR1; full-length interferon (IFN)-inducible ADAR1p150 (top) and a constitutive ADAR1p110 form (middle). Z-DNA binding domain, black; dsRNA Binding Domain (dsRBD), blue; deaminase domain, pink; nuclear Localization Signal (NLS), green; catalytic core (E861), dark blue diamond. A 400aa murine ADAR1 epitope (bottom) with an amino-terminal HIS tag was used to immunize rats for monoclonal antibody production. **C**) Western blot (WB) of E12.5 brain, whole embryo and P1 MEFs from *Adar1*$^{+/+}$, *Adar1*$^{E861A/+}$ and *Adar1*$^{E861A/E861A}$ probed with anti-ADAR1 mAb (top) and the same blot re-probed with anti-βACTIN (bottom). Black rectangles indicate regions cropped for Fig. 1C. **D**) Representative images of E12.5 embryo proper of respective genotypes. **E)** FL cellularity at E12.5 and E13.5. **F)** Western blot of E11 *Adar1*$^{+/-}$ and *Adar1*$^{-/-}$ embryos, *Adar1*$^{E861A/+}$ and *Adar1*$^{E861A/E861A}$ from E12.5 passage 1 (P1) MEFs and brain, probed with anti-ADAR1 monoclonal antibody (mAb, top) and anti-αTUBULIN (bottom). Results are expressed the mean±SEM (E12.5, *Adar1*$^{+/+}$ n=5, *Adar1*$^{E861A/+}$ n=22 and *Adar1*$^{E861A/E861A}$ n=13; E13.5, *Adar1*$^{+/+}$ n=5, *Adar1*$^{E861A/+}$ n=18 and *Adar1*$^{E861A/E861A}$ n=3). Significance was assessed compared to *Adar1*$^{+/+}$.

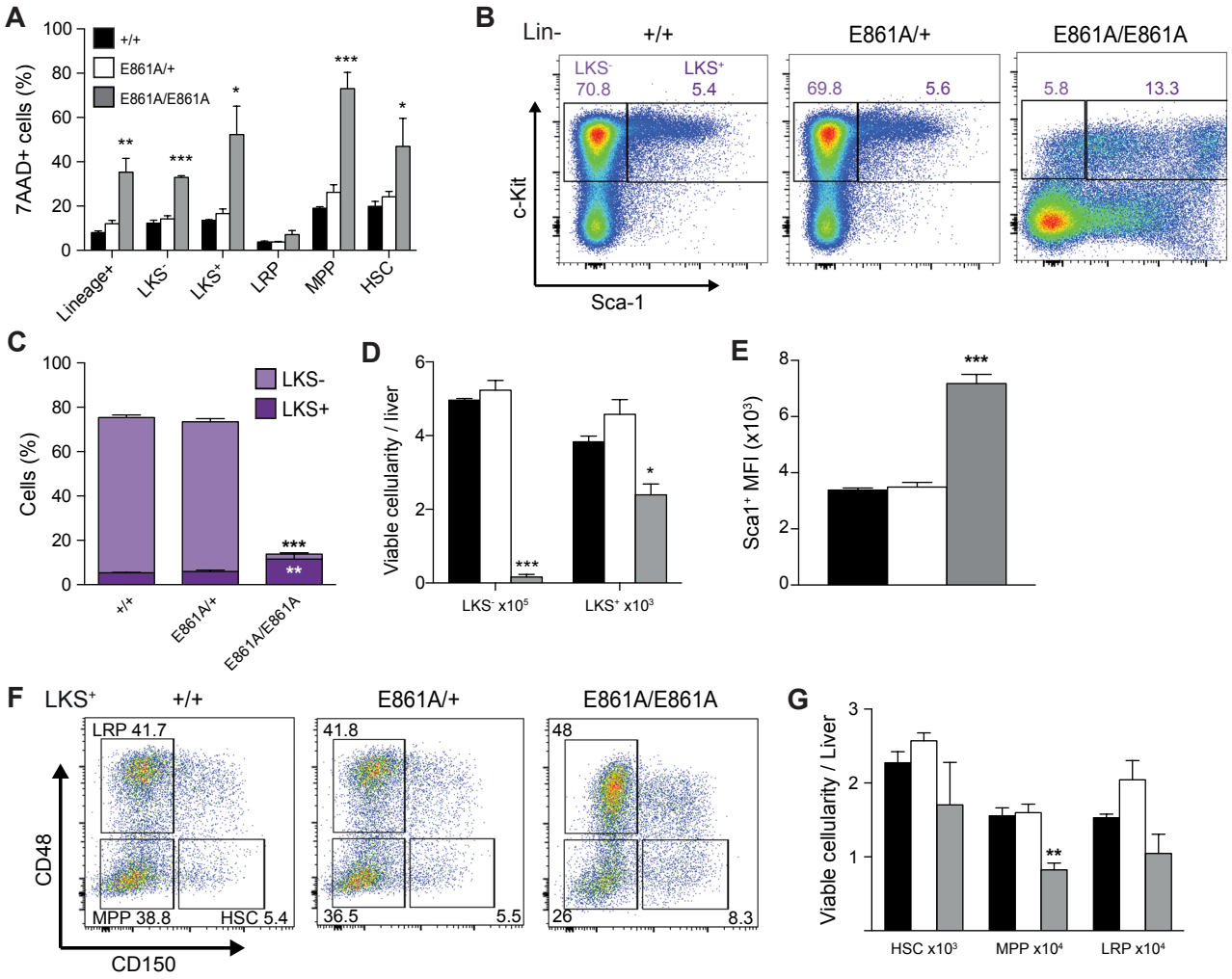
A
7AAD+ cells (%)
+/+
E861A/+
E861A/E861A
Lineage+
LKS-
LKS+
LRP
MPP
HSC
B
Lin-
+/+
E861A/+
E861A/E861A
LKS-
LKS+
70.8
5.4
69.8
5.6
5.8
13.3
c-Kit
Sca-1
C
Cells (%)
LKS-
LKS+
D
Viable cellularity / liver
LKS- x10^5
LKS+ x10^3
E
Sca1+ MFI (x10^3)
F
LKS+
+/+
E861A/+
E861A/E861A
LRP 41.7
41.8
48
MPP 38.8
HSC 5.4
36.5
5.5
26
8.3
CD48
CD150
G
Viable cellularity / Liver
HSC x10^3
MPP x10^4
LRP x10^4
H
Colonies
BFU-E
CFU-GEMM
CFU-GM
+/+
E861A/+
E861A/E861A
Genotype
I
+/+
E861A/+
E861A/E861A
CFC
GM

Figure S2. Failed hematopoiesis in *Adar1*$^{E861A/E861A}$ embryos

E13.5 fetal liver **A**) frequency of dead (7AAD+) mature leukocytes (Lineage+), lineage-c-Kit+Sca1- (LKS-), lineage-c-Kit+Sca1+ (LKS+), lineage restricted progenitors (LRP), multipotent progenitors (MPP) and hematopoietic stem cells (HSC) in *Adar1*$^{+/+}$ (+/+, black bars), *Adar1*$^{E861A/+}$ (E861A/+, white bars) and *Adar1*$^{E861A/E861A}$ (E861A/E861A, grey bars). **B**) Representative FACs plots, **C)** frequency and **D)** total viable cellularity of LKS^{-} progenitors and LKS^{+} stem cells. **E**) Mean fluorescence intensity (MFI) of Sca1^{+} expression, determine by flow cytometry. **F)** Representative FACs plots and **G)** total viable cellularity of LRP, MPP and HSCs, determined by CD48 and CD150 expression of LKS^{+} fraction. Results are depicted as mean±SEM (+/+ n=4, E861A/+ n=12 and E861A/E861A n=3). *p<0.05, **p<0.005 and ***p<0.0005 compared to +/+. E12.5 FL **H**) Numbers of burst-forming unit erythroid (BFU-E); colony-forming unit (CFU); CFU-GEMM, granulocyte-erythrocyte-monocyte-macrophage; CFU-GM, granulocyte-monocyte and **I**) representative images of E12.5 FL colonies (Top, whole plate, 10x magnification; bottom, CFU-GM colonies, 40x magnification, scale bar = 2mm). Results are mean±SEM (+/+ n=3, E861A/+ n=13 and E861A/E861A n=6). **p<0.005 and ***p<0.0005 compared to *Adar1*$^{+/+}$ controls.

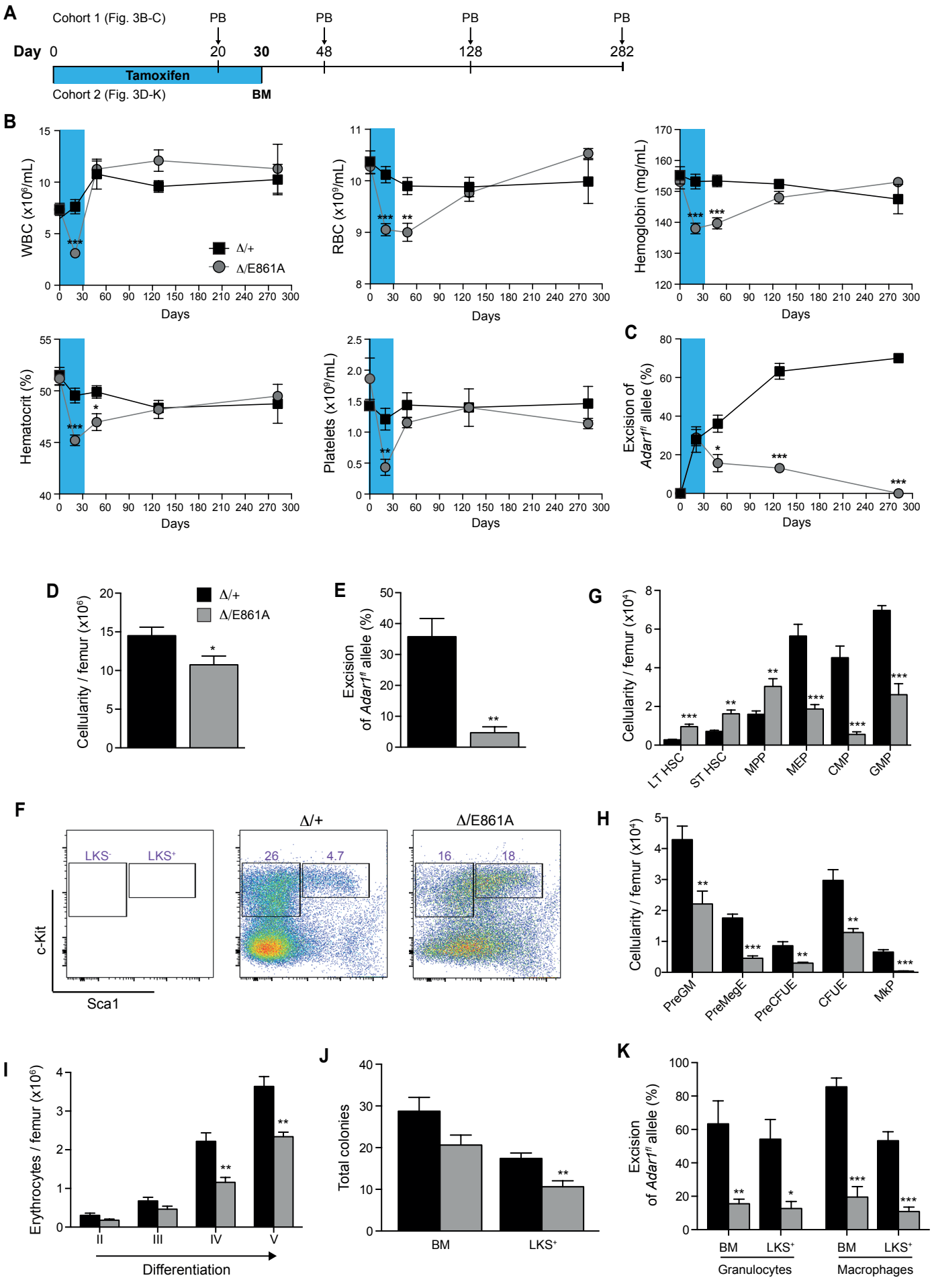
A
Cohort 1 (Fig. 3B-C)
PB
PB
PB
PB
Day 0
20
30
48
128
282
Tamoxifen
Cohort 2 (Fig. 3D-K)
BM
B
WBC (x10⁶/mL)
RBC (x10⁹/mL)
Hemoglobin (mg/mL)
Hematocrit (%)
Platelets (x10⁹/mL)
Days
Δ/+
Δ/E861A
C
Excision of Adar1fl allele (%)
D
Cellularity / femur (x10⁶)
E
Excision of Adar1fl allele (%)
G
Cellularity / femur (x10⁴)
LT HSC
ST HSC
MPP
MEP
CMP
GMP
F
Δ/+
Δ/E861A
LKS⁻
LKS⁺
26
4.7
16
18
c-Kit
Sca1
H
Cellularity / femur (x10⁴)
PreGM
PreMegE
PreCFUE
CFUE
MkP
I
Erythrocytes / femur (x10⁶)
II
III
IV
V
Differentiation
J
Total colonies
BM
LKS⁺
K
Excision of Adar1fl allele (%)
BM
LKS⁺
BM
LKS⁺
Granulocytes
Macrophages

Figure S3. ADAR1-mediated editing is required to maintain adult hematopoiesis

A) Experimental outline for *hScl-Cre*ER^{T}*Adar1*$^{fl/E861A}$ (Δ/E861A) and control *hScl-Cre*ER^{T}*Adar1*$^{fl/+}$ (Δ/+) mice. Mice were placed on a tamoxifen diet (blue shaded area) for 30 days and PB was analyzed at days 20, 48, 128 and 282. **B**) PB leukocyte (WBC) and red blood cell (RBC) indices, hemoglobin, hematocrit and platelet counts. **C**) Excision efficiency of the *Adar1*^{fl} allele in PB. Results are mean±SEM (Δ/E861A n=6 and Δ/+ n=5). Analysis of BM **D**) cellularity and **E**) excision efficiency of the *Adar1*^{fl} allele after 30-days of tamoxifen diet. **F**) Representative FACS plots of LT-HSC, ST-HSC and MPP populations within LKS^{+} fraction. **G**) Numbers of long-term (LT-HSC) and short term (ST-HSC) repopulating HSCs, multipotent progenitors (MPP) and myeloid progenitor populations (CMP = common myeloid progenitor; GMP = granulocyte macrophage progenitor; MEP = megakaryocyte erythroid progenitor) per femur. **H**) Numbers of myeloerythroid progenitors; PreGM, PreMegE, PreCFUE, CFUE and MkP per femur. **I**) Analysis of erythroid differentiaion in Δ/E861A and control mice. **J**) CFU frequency from 5x10^{4} BM and 500 primary isolated LKS^{+} cells from Δ/E861A and control mice. **K**) *Adar1*^{fl} allele excision efficiency in granulocyte and macrophage CFU from BM and LKS^{+} colonies. Results are mean±SEM (Δ/E861A n=4 and Δ/+ n=6). *p<0.05, **p<0.005 and ***p<0.0005 compared to Δ/+.

Liddicoat et al., Supplemental Figure S4

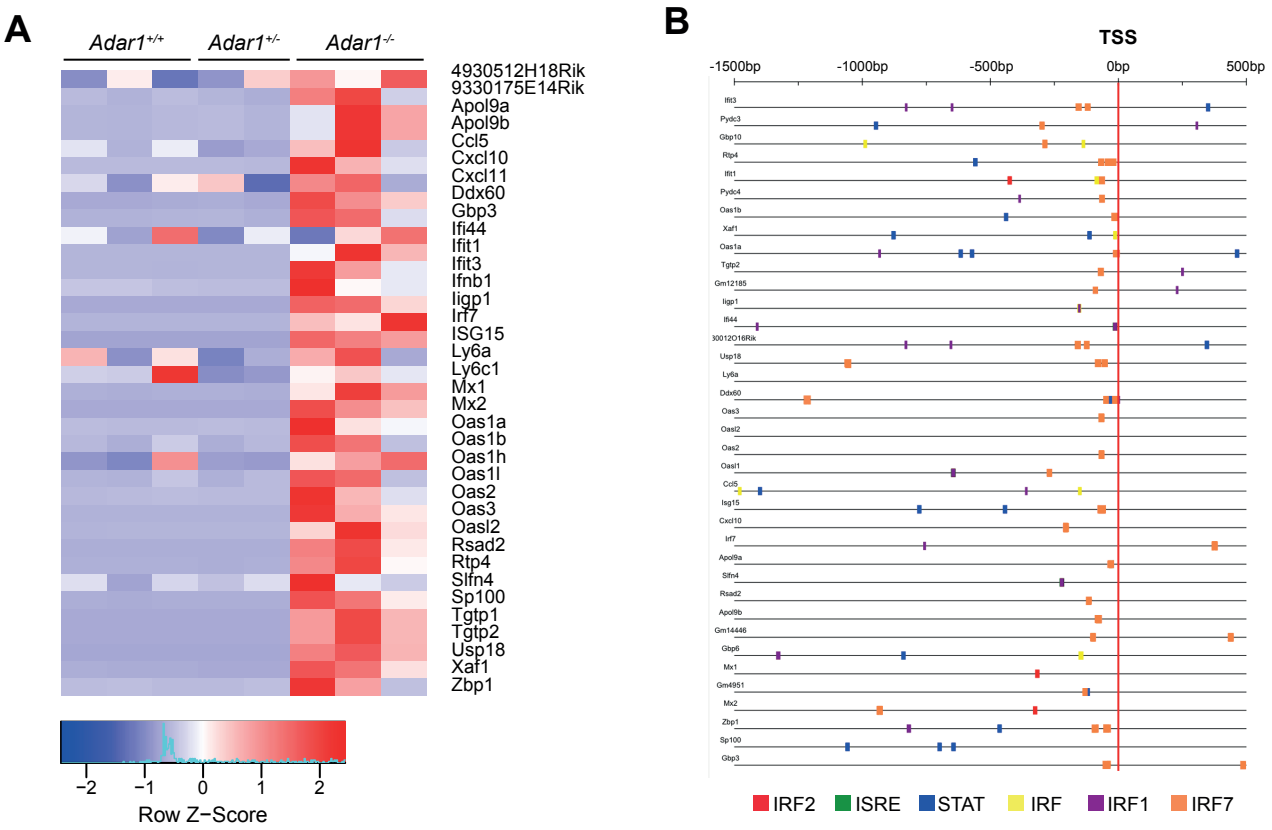

Figure S4. Specific loss of ADAR1 mediated A-to-I editing transcriptionally phenocopies loss of ADAR1

Analysis of the top 50 most differentially expressed genes in *Adar1*$^{E861A/E861A}$ compared to *Adar1*$^{+/+}$ E12.5 FL. **A**) Heatmap of 36 ISGs annotated in GSE12772 data set (14 were not annotated) of *Adar1*$^{-/-}$ compared to *Adar1*$^{+/+}$ and *Adar1*$^{+/-}$ control HSCs. **B**) Transcription factor binding sites (TFBS) for 33 ISGs (TFBS have yet to be determined for remaining 17 transcripts), red line indicates transcription start site (TSS). Data derived from Interferome v2.01 database.

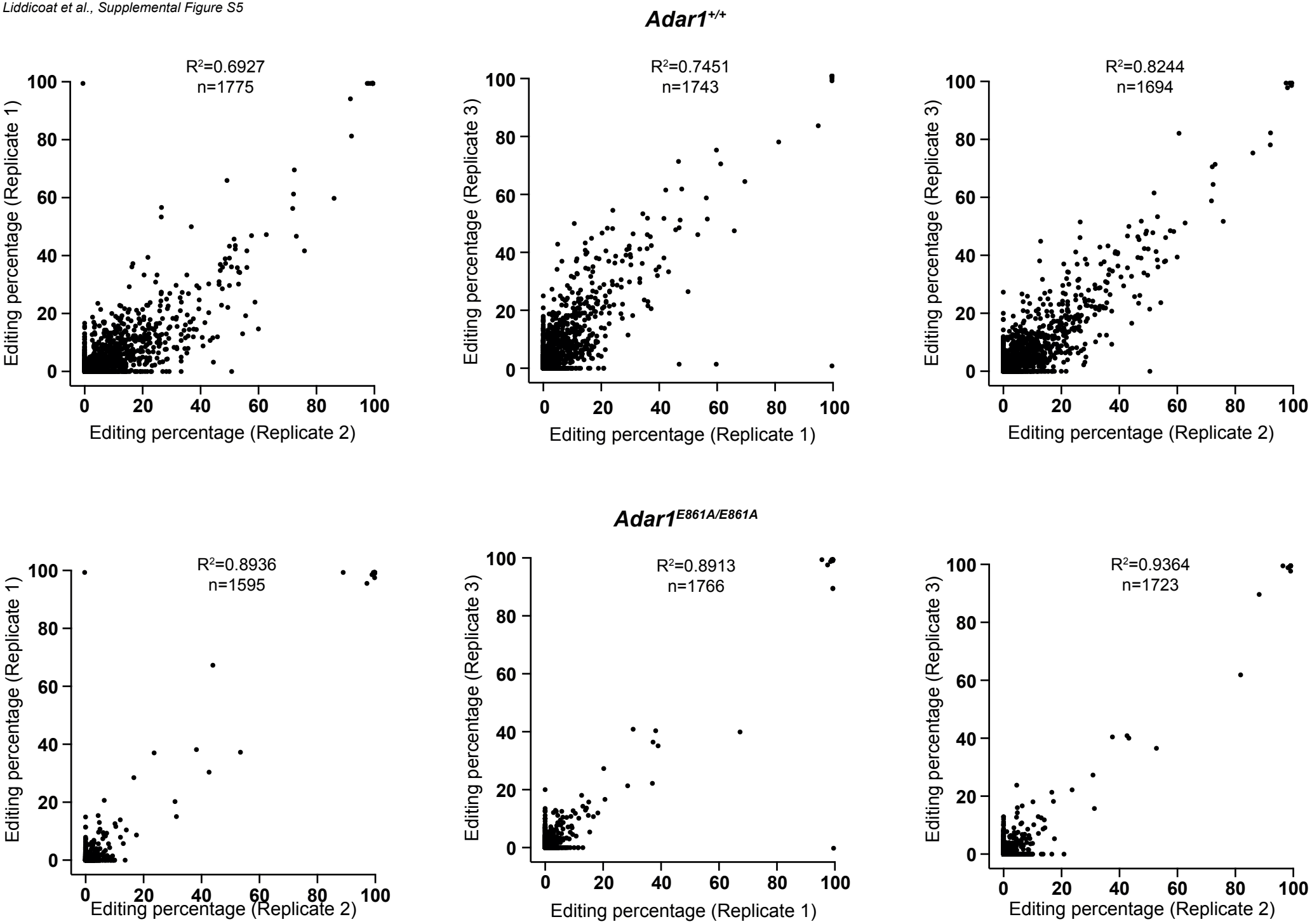
Adar1+/+
R2=0.6927
n=1775
Editing percentage (Replicate 1)
Editing percentage (Replicate 2)
R2=0.7451
n=1743
Editing percentage (Replicate 3)
Editing percentage (Replicate 1)
R2=0.8244
n=1694
Editing percentage (Replicate 3)
Editing percentage (Replicate 2)
Adar1E861A/E861A
R2=0.8936
n=1595
Editing percentage (Replicate 1)
Editing percentage (Replicate 2)
R2=0.8913
n=1766
Editing percentage (Replicate 3)
Editing percentage (Replicate 1)
R2=0.9364
n=1723
Editing percentage (Replicate 3)
Editing percentage (Replicate 2)

Figure S5. A-to-I editing sites with >20reads coverage

Scatterplots of A-to-I editing frequencies between *Adar1*$^{+/+}$ (top) and *Adar1*$^{E861A/E861A}$ (bottom) independent biological triplicates from E12.5 FL RNA-seq.

Liddicoat et al., Supplemental Figure S6

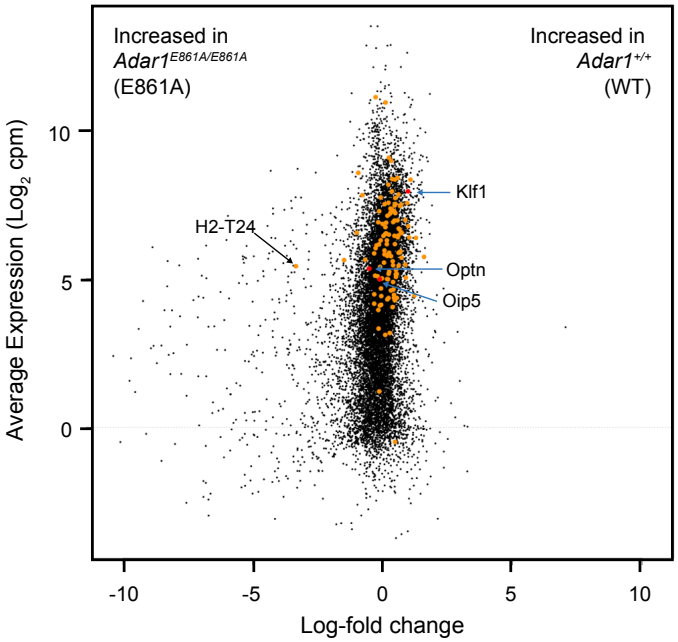

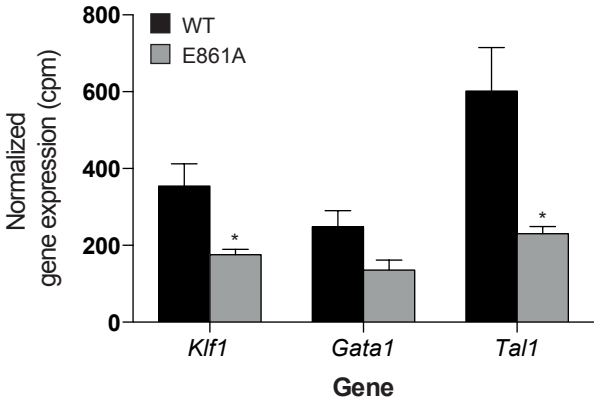

Figure S6. Expression of hyper-edited substrates in FL

A) MA plot comparing gene expression, Data expressed as average gene expression (Log_2 cpm) on the Y axis, Log-fold change (Log_2) on the X-axis with direction of enrichment as indicated. Orange dots indicate edited transcripts and red dots mark the hyper-edited transcripts *Klf1*, *Optn* and *Oip5*. **B)** Normalized expression of the erythroid transcription factors *Klf1*, *Gata1* and *Tal1*. Data expressed as mean normalized gene expression (cpm)±SEM, *$p<0.05$. Data from 3 independent biological samples of each genotype, RNA-seq from E12.5 whole FL.

A *Klf1: ΔG = -1724.55*

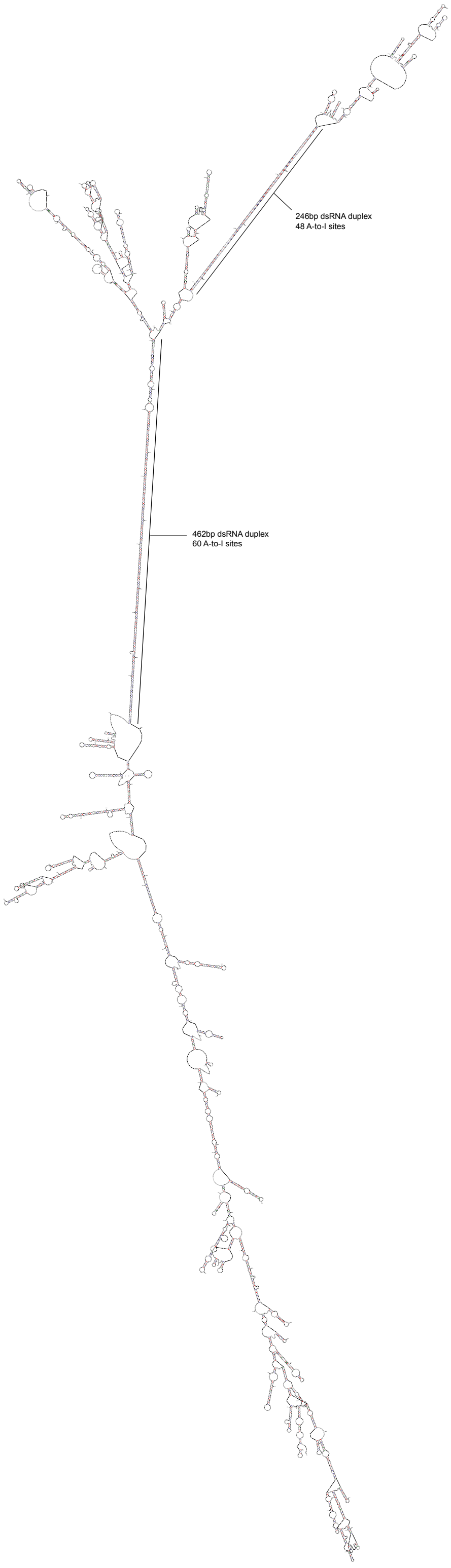

B

Oip5: ΔG = -808.83

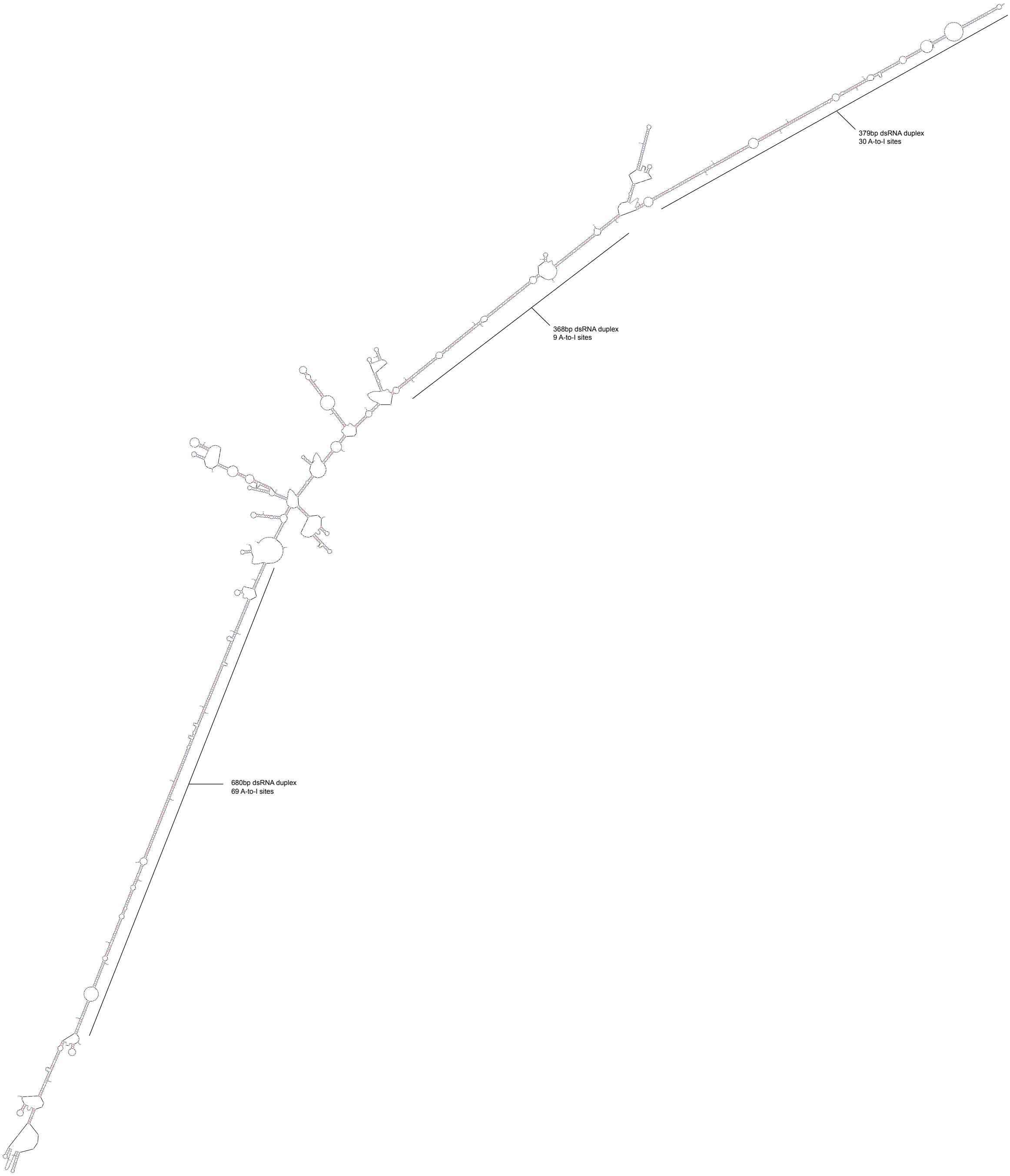

C

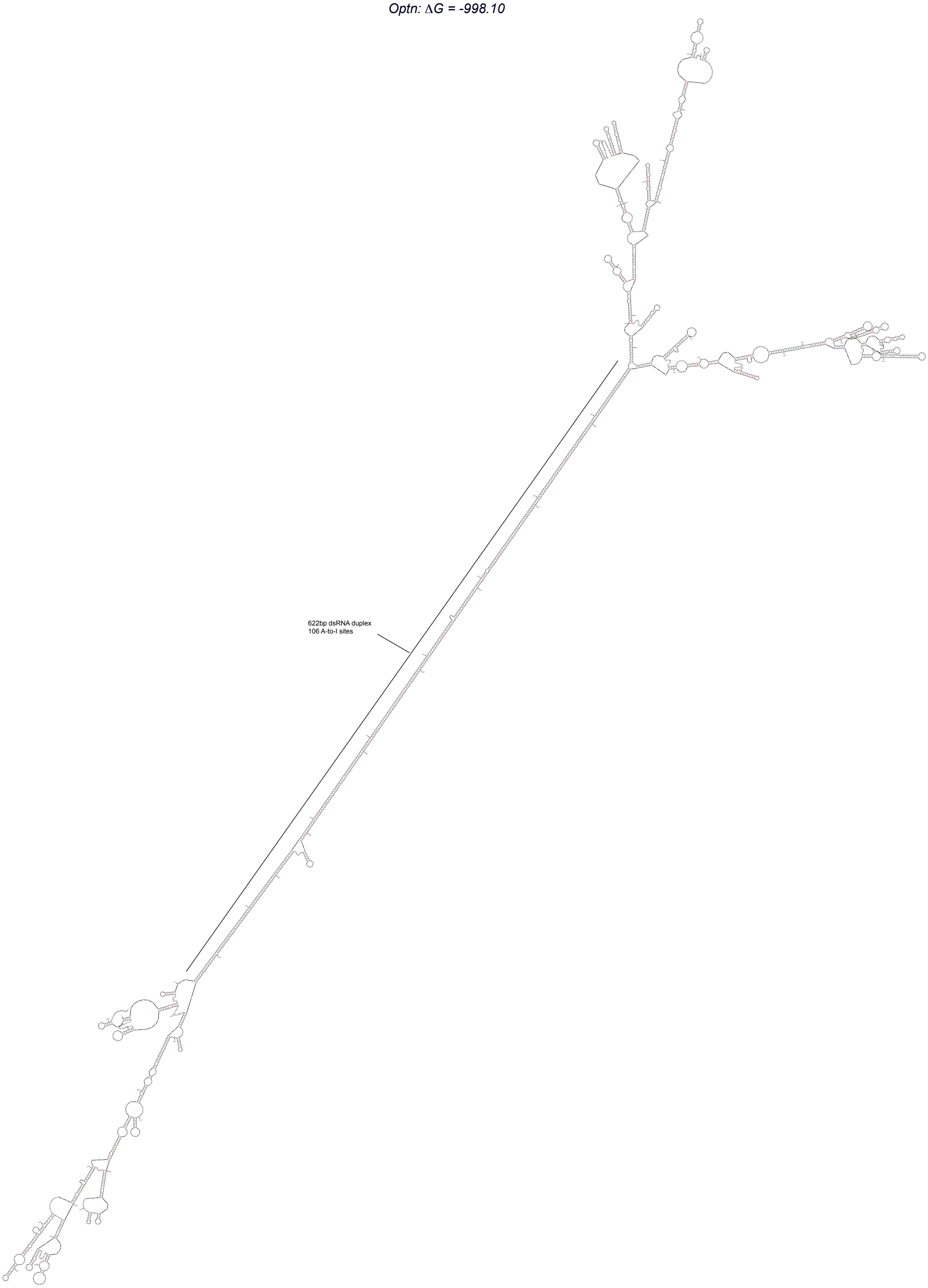

D *Klf1 (edited): ΔG = -1342.05*

E

Oip5 (Edited): ΔG = -604.21

F

Optn (Edited): ΔG = -681.31

G

Pum2: ΔG = -618.09

H

Ppp1r15b: ΔG = -870.15

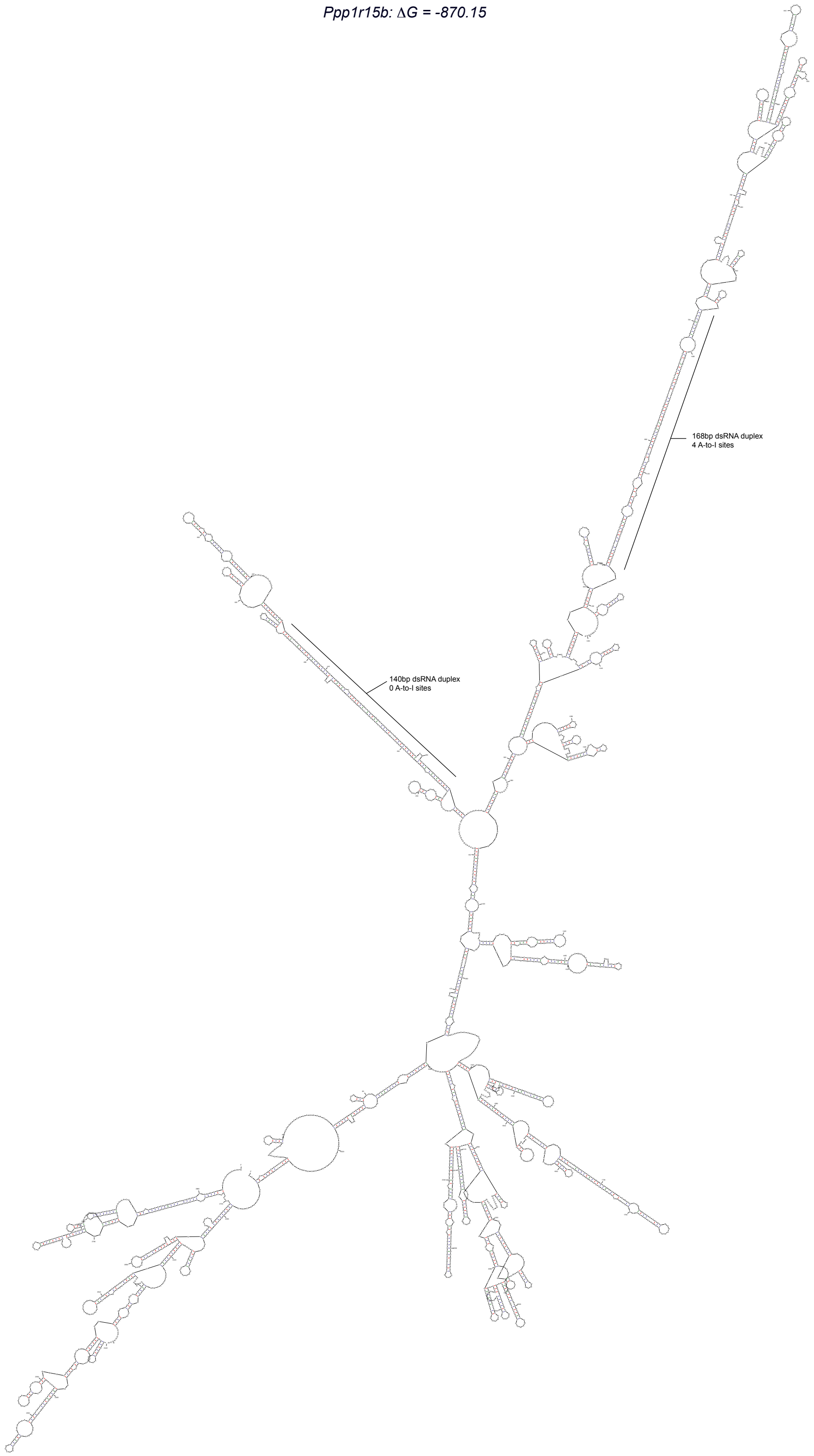

I

Malt1: ΔG = -639.64

Figure S7. RNA secondary structures of ADAR1 edited transcripts

Predicted secondary structure of non-edited (genomic encoded sequence) 3' UTRs of **A**) *Klf1* **B**) *Oip5* and **C**) *Optn* and hyperedited (sequence based on A-to-I editing sites identified in RNA-seq dataset) 3' UTRs of **D**) *Klf1* **E**) *Oip5* and **F**) *Optn*. Predicted secondary structure of non-edited (genomic encoded sequence) 3' UTRs of **G**) *Pum2* **H**) *Ppp1r15b* and **I**) *Malt1*. Length of defined dsRNA duplex regions are represented as the number of nucleotide bases in the duplex and the number of A-to-I editing sites in each respective duplexes are defined. Free energy states of each structure is depicted as ΔG.

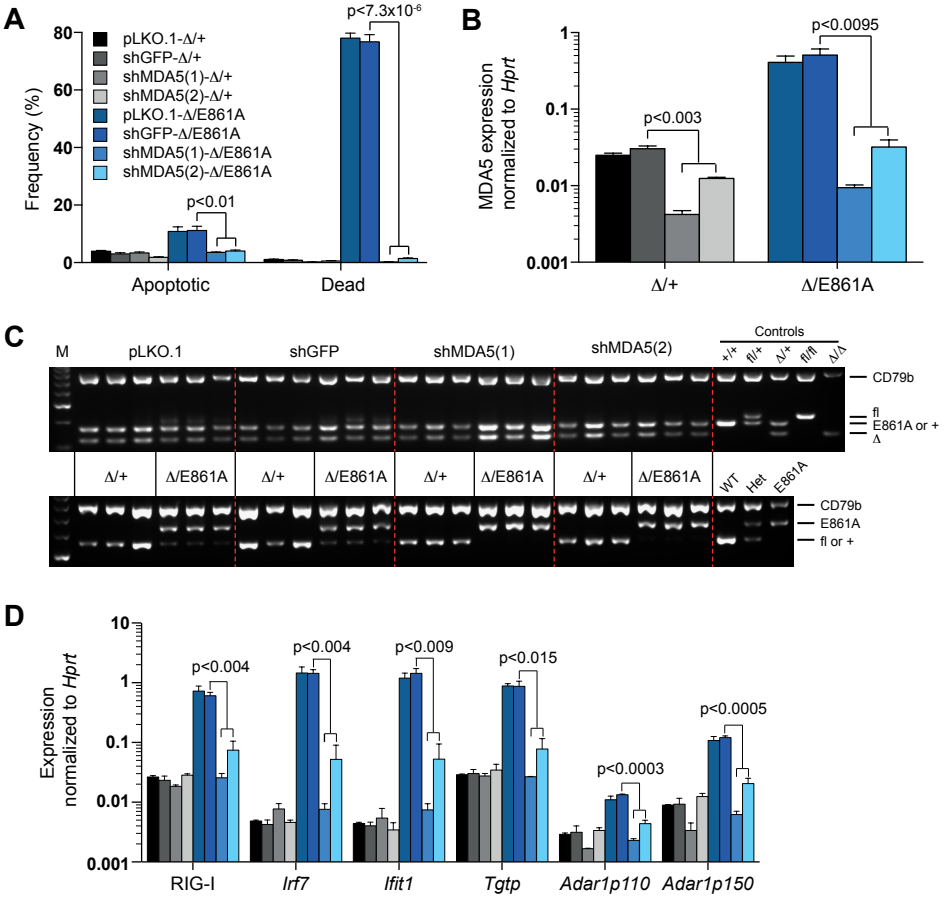
A
Frequency (%)
pLKO.1-Δ/+
shGFP-Δ/+
shMDA5(1)-Δ/+
shMDA5(2)-Δ/+
pLKO.1-Δ/E861A
shGFP-Δ/E861A
shMDA5(1)-Δ/E861A
shMDA5(2)-Δ/E861A
p<0.01
p<7.3x10-6
Apoptotic
Dead
B
MDA5 expression normalized to Hprt
p<0.003
p<0.0095
Δ/+
Δ/E861A
C
M
pLKO.1
shGFP
shMDA5(1)
shMDA5(2)
Controls
+/+
fl/+
Δ/+
fl/fl
Δ/Δ
CD79b
fl
E861A or +
Δ
Δ/+
Δ/E861A
WT
Het
E861A
CD79b
E861A
fl or +
D
Expression normalized to Hprt
p<0.004
p<0.004
p<0.009
p<0.015
p<0.0003
p<0.0005
RIG-I
Irf7
Ifit1
Tgtp
Adar1p110
Adar1p150

Figure S8. MDA5 knock-down rescues ADAR1 editing deficient hematopoietic cells

LKS^{+} cells were isolated from *Rosa26*CreER^{T2} *Adar1*$^{fl/+}$ (Δ/+) and *Rosa26*CreER^{T2} *Adar1*$^{fl/E861A}$ (Δ/E861A) infected with pLKO.1 empty vector, shGFP or two independent shMDA5 (shMDA5(1) and shMDA5(2)) were cultured for 8 days with 500nM tamoxifen after puromycin selection. **A)** Frequency of apoptotic (AnnexinV+/7AAD-) and dead (AnnexinV+7AAD+) cells after 8 days in culture. **B)** RT-qPCR of MDA5 expression in control and shMDA5 knockdown cells at day 5. **C)** Genomic DNA PCR of *Adar1*^{fl} excision (top) and genotype (bottom). CD79b is a loading control. **D**) RT-qPCR of ISG and *Adar1* expression in control and shMDA5 knockdown cells at day 5. Results are mean±SEM (n=3 independent experiments). *P*-values indicative of significant difference between shMDA5(1) and shMDA5(2), and shGFP within genotypes.

A

Adar1$^{E861A/+}$*Ifih1*$^{-/-}$ X *Adar1*$^{E861A/+}$*Ifih1*$^{-/-}$				
		Ifih1$^{-/-}$		
Stage	**Litters**	**+/+**	**E861A/+**	**E861A/E861A**
E13.5	2	2	8	4
Expected		3.5	7	3.5

B

Adar1$^{E861A/+}$*Ifih1*$^{+/-}$ X *Adar1*$^{E861A/+}$*Ifih1*$^{+/-}$ (12 litters)		
Genotype	**Observed**	**Expected**
Adar1$^{+/+}$*Ifih1*$^{+/+}$	8	4 (6.3%)
Adar1$^{+/+}$*Ifih1*$^{+/-}$	14	8 (12.5%)
Adar1$^{+/+}$*Ifih1*$^{-/-}$	7	4 (6.3%)
Adar1$^{E861A/+}$*Ifih1*$^{+/+}$	9	8 (12.5%)
Adar1$^{E861A/+}$*Ifih1*$^{+/-}$	18	16 (25%)
Adar1$^{E861A/+}$*Ifih1*$^{-/-}$	6	8 (12.5%)
Adar1$^{E861A/E861A}$*Ifih1*$^{+/+}$	0	4 (6.3%)
Adar1$^{E861A/E861A}$*Ifih1*$^{+/-}$	0	8 (12.5%)
Adar1$^{E861A/E861A}$*Ifih1*$^{-/-}$	2	4 (6.3%)

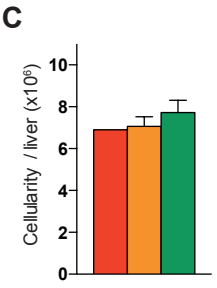

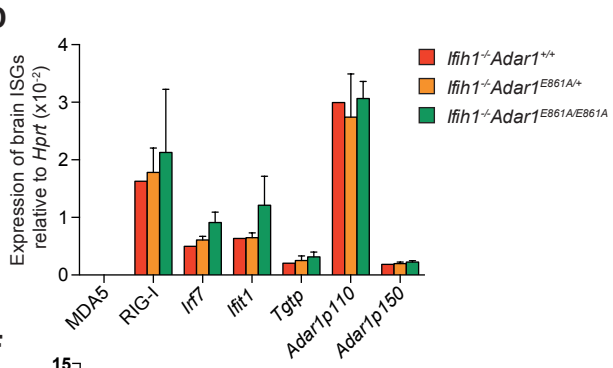

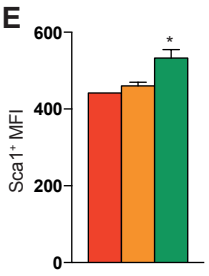

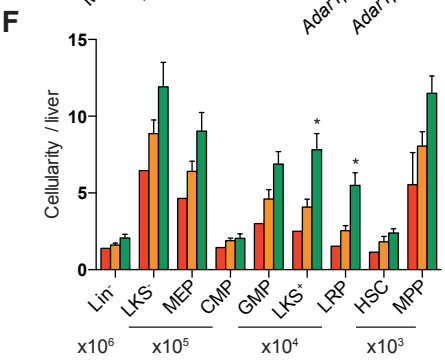

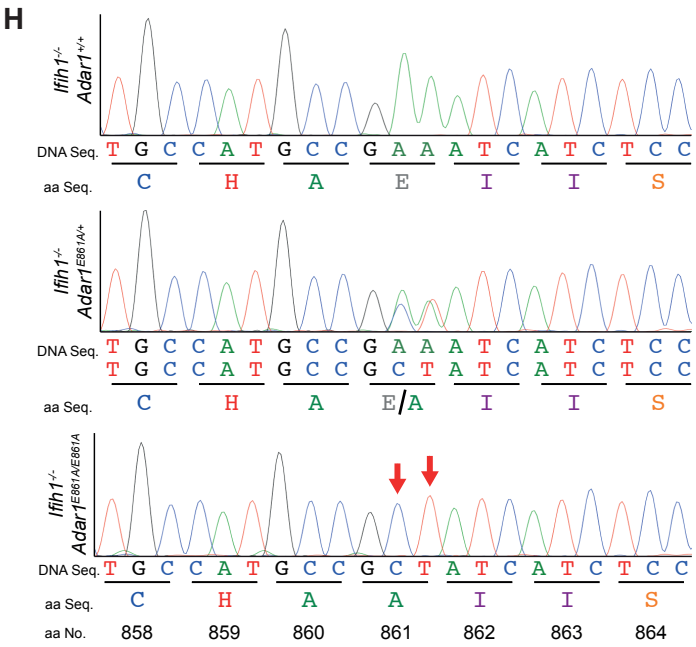

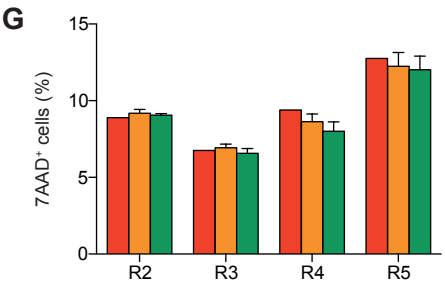

Figure S9. MDA5 knock-out rescues ADAR1 editing deficient embryonic death

A) 7 week old *Adar1*$^{E861A/+}$*Ifih1*$^{-/-}$ mice were intercrossed. Table of observed *Adar1* genotypes at E13.5 from timed plug matings. All embryos are *Ifih1*$^{-/-}$. **B)** Table of observed and expected genotypes from *Adar1*$^{E861A/+}$*Ifih1*$^{+/-}$ intercrosses (double heterozygous). **C)** FL cellularity, **D)** ISG and **E)** Sca1 surface expression at E13.5 of indicated genotypes. **F)** Enumeration of hematopoietic fractions. See Fig. S2-S3 for details of populations. G) Frequency of 7AAD^{+} erythroid cells. Results are mean±SEM (+/+, n=2; E861A/+, n=8; E861A/E861A, n=4). *$p<0.05$ compared to *Adar1*$^{+/+}$*Ifih1*$^{-/-}$ controls. **H**) Exon 9 of *Adar1* was PCR amplified and Sanger sequencing traces for respective genotypes are depicted (gDNA) from viable pups identified at day 10 by genotyping.

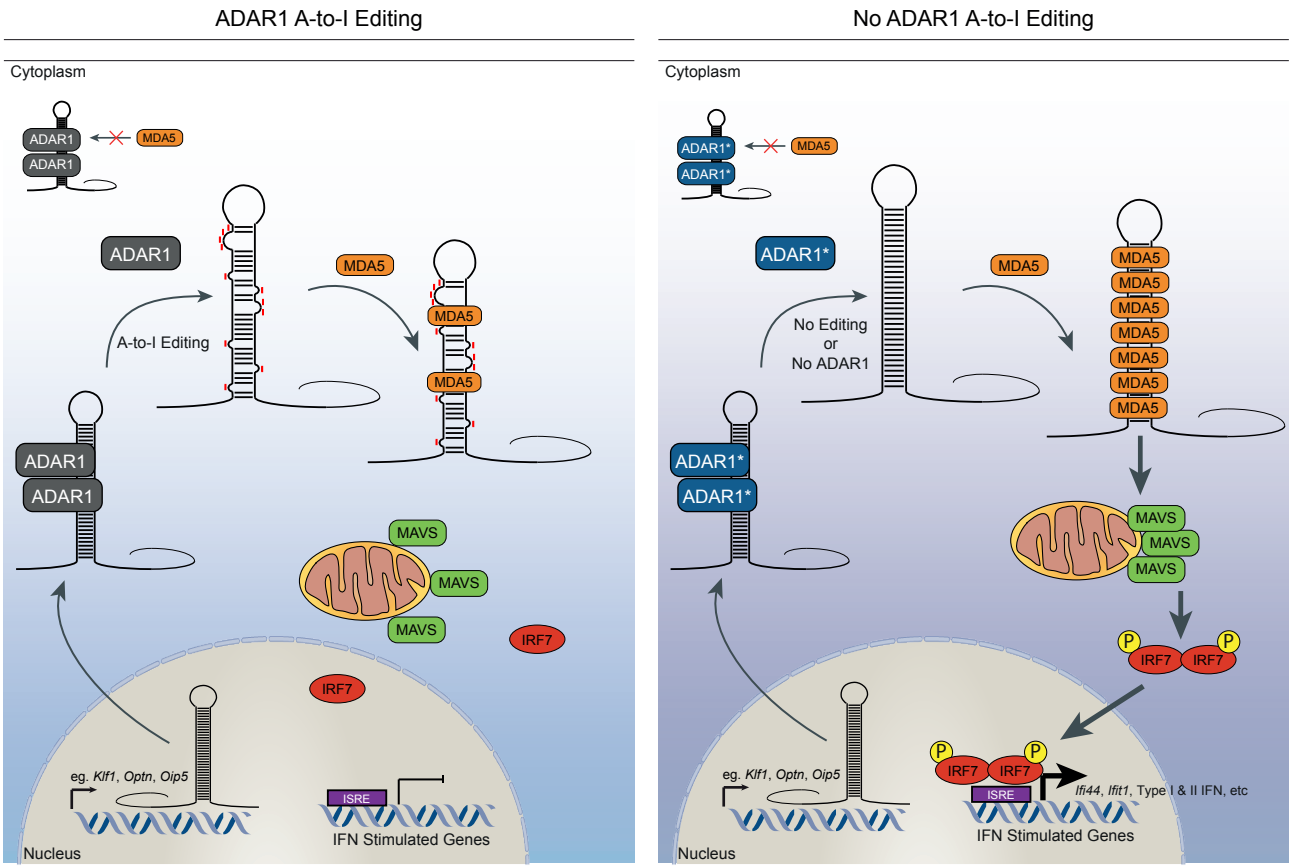
ADAR1 A-to-I Editing
No ADAR1 A-to-I Editing
Cytoplasm
Cytoplasm
ADAR1
ADAR1
MDA5
ADAR1
A-to-I Editing
MDA5
MDA5
MDA5
ADAR1
ADAR1
MAVS
MAVS
MAVS
IRF7
IRF7
eg. Klf1, Optn, Oip5
ISRE
IFN Stimulated Genes
Nucleus
ADAR1*
ADAR1*
MDA5
ADAR1*
No Editing
or
No ADAR1
MDA5
MDA5
MDA5
MDA5
MDA5
MDA5
MDA5
ADAR1*
ADAR1*
MAVS
MAVS
MAVS
P
IRF7
IRF7
P
eg. Klf1, Optn, Oip5
P
IRF7
IRF7
P
ISRE
Ifi44, Ifit1, Type I & II IFN, etc
IFN Stimulated Genes
Nucleus

Figure S10. Proposed model for ADAR1 action and consequences of lack of editing

Proposed model for ADAR1-mediated A-to-I editing. IU-dsRNA mismatches prevent MDA5 oligomerization and downstream ISG transcription (left). In the absence of ADAR1-mediated hyper-editing, MDA5 oligomerizes along self-dsRNA and upregulates ISGs via MAVS and IRF7.

Additional Data Tables (separate excel files)

Table S1 Gene expression profiles of ADAR1 wild-type and mutant E12.5 fetal liver

Table S2 Identification of fetal liver A-to-I editing sites

Table S3 Hyperediting analysis of E12.5 fetal liver

Table S4 mmPCR-Seq validation of high confidence editing sites